

THE INFLUENCE OF STELLAR OBJECTS MASS DISTRIBUTION ON THEIR GRAVITATIONAL FIELDS

Vladimir Stephanovich,¹ Włodzimierz Godłowski,¹ Monika Biernacka,² and
Błażej Mrzygłód,¹

Draft version: November 5, 2021

RESUMEN

ABSTRACT

We study the influence of the astronomical objects masses randomness on the distribution function of their gravitational fields. Based on purely theoretical arguments and comparison with extensive data, collected from observations and numerical simulations, we have shown that while mass randomness does not alter the non-Gaussian character of the gravitational fields distribution, it changes the dependencies of mean angular momenta of galaxies and clusters on their richness. The specific form of above dependence is determined by the interplay of mass distribution character and different assumptions about cluster morphology. We trace the influence of masses distribution on the time evolution of stellar objects angular momenta in CDM and Λ CDM models. Our theoretical predictions are in very good coincidence with the statistical results derived both from observational data and numerical simulations.

Key Words: Galaxy:General — Galaxy:Formation

1. INTRODUCTION

As the gravitational fields are highly nonuniform during galaxies and their clusters formation, the distribution of former plays an important role. Moreover, the character of gravitational field distribution permits to discern the specific scenario of galaxies formation. The classical scenarios of such formation had been proposed quite long time ago (Peebles 1969; Zeldovich 1970; Sunyaew & Zeldovich 1972; Doroshkevich 1973; Shandarin 1974; Efstathiou & Silk 1983; Dekel 1985) and dealt primarily with so-called Zeldovich pancake model (Zeldovich 1970), based on large gravitating body (of the pancake shape, hence the name) mechanical instability without any randomness in gravitational fields of the constituents (Zeldovich 1970; Shandarin & Zeldovich 1989; Longair 2008). These classical scenarios have not lost significance till now as new scenarios are essentially modifications of the classical ones and can be classified according to them. The improved form of the above classical scenarios has been put forward more recently, see (Shandarin et al 2012; Giah-Saravani & Schäfer 2014) for relevant references. The presence or absence of the random gravitational field fluctuations contribute to the studies of galaxies angular momentum acquisition during their formation stages. This may in principle permit to specify the most probable (among many other) scenario of the large stellar

¹Uniwersytet Opolski, Institute of Physics, ul. Oleska 48, 45-052 Opole, Poland.

²Institute of Physics, Jan Kochanowski University, ul. Świetokrzyska 15, 25-406 Kielce, Poland.

objects emergence. This is because the final test of a given scenario correctness is the comparison of its predictions with observations. The investigations of the variations of structures angular momenta gives us the opportunity to do so. Note that different scenarios make different predictions about galaxies orientations, i.e. their angular momenta alignments in structures (Peebles 1969; Doroshkevich 1973; Shandarin 1974; Efsthathiou & Silk 1983; Catelan & Theuns 1996; Li 1998; Lee & Pen 2000, 2001; Lee & Pen 2002; Navarro et al. 2004; Trujillio et al. 2006; Zhang et al. 2013). For this reason the analysis of galaxies planes orientation is regarded as a standard test of different scenarios of the cosmic structures formation (Romanowsky & Fall 2012; Joachimi et al. 2015; Kiessling et al. 2015).

One of the natural sources of gravitational fields randomness is the masses distribution of stellar objects. The simplest possible model of the masses distribution dates back to (Chandrasekhar 1943), where the *a priori* given distribution function of masses $\tau(M)$ has been considered. In this paper, all characteristics of the stellar ensemble has been expressed through the different average powers of mass. The mass averaging had there been performed implicitly with the above function $\tau(M)$. In principle, such approach can be generalized to the averaging over quadrupole and higher multipole moments of galaxies in the spirit of the (Stephanovich & Godłowski 2015). Although this effect may change some of the results quantitatively, we speculate that its overall influence will be rather faint. Next step has been done by (Press & Schechter 1974), who considered the distribution function of stellar objects masses within the model of self-similar gravitational condensation. In this work, within the model of the expanding Universe in Friedmann cosmology, the stellar ensembles had been represented as a "gas" of self-gravitating masses, which can condense into aggregates with larger mass, forming finally very large clumpy objects. This model permits to derive the distribution of masses in the form

$$f(m) = A \left(\frac{m}{m_*} \right)^\alpha e^{-m/m_*}, \quad (1)$$

where A is a normalization constant, see below. Note that the explicit expression of Shechter function (1) has been listed in the work (Schechter 1976) devoted to the luminosity distribution of galaxies. Below we will use function (1) for the calculation of the amended (on the mass distribution) distribution function of the gravitational fields and angular momenta. Using this function, we assume that the mass is proportional to the first degree of a luminosity: $m \sim L$. Below we give the arguments why possible nonlinearity $m \sim L^\gamma$ ($\gamma \neq 1$) will not change our results qualitatively.

In the present paper, we consider tidal interaction in the ensemble of galaxies and their clusters in a Friedmann-Lemaître-Robertson-Walker Universe with Newtonian self-gravitating dust fluid ($p = 0$) containing both luminous and dark matter. The commonly accepted model of such Universe is spatially flat homogeneous and isotropic Λ CDM model. The clumpy objects like galaxies and their clusters are formed as a result of almost scale invariant Gaussian fluctuations (Silk 1968; Peebles & Yu 1970; Sunyaew & Zeldovich 1970). This assumption is the base of the so-called hierarchical clustering model (Doroshkevich 1970; Dekel 1985; Peebles 1969). The models with non-Gaussian initial fluctuations have also been considered

in (Bartolo et al 2004). The non-Gaussian character of distribution function has been postulated there, rather than calculated. Such calculation has been presented in (Stephanovich & Godłowski 2015, 2017), where the non-Gaussian distribution of gravitational fields and momenta were calculated using method of (Chandrasekhar 1943). Here we generalize this calculation considering the masses distribution (1). Note that the calculations made in (Stephanovich & Godłowski 2015, 2017) dealt with equilibrium situation only. To consider non-equilibrium situation, it is necessary to use the differential equations of Fokker-Planck type with so-called fractional derivatives (Garbaczewski & Stephanovich 2009, 2011). In this case we can begin with ubiquitous Gaussian distribution and arrive at a non-Gaussian one as a result of primordial, fast time evolution. After it, the slower evolution, dictated by the Λ CDM scenario, takes place. Note that recently time evolution of intrinsic galaxies alignments has been found by (Schmitz et al. 2018).

In hierarchical clustering approach, the large clumpy structures form as a result of gravitational interactions between smaller objects. In other words, the galaxies spin angular momenta arise as a result of tidal interaction with their neighbors (Schäfer 2009). Note, that in the present paper the angular momentum is the result of tidal interaction with the entire environment, which occurs via interaction transfer from close to distant galaxies, see below. That is to say that our approach is the generalization of (Schäfer & Merkel 2012; Catelan & Theuns 1996,a; Lee & Pen 2002), where the average tidal interaction with the entire environment has been considered. In the present work we perform the theoretical and statistical analysis of the influence of tidal interaction between astronomical objects on the larger (then initial constituents) structures formation. We have also performed the comparison of our model predictions with vast data arrays, derived from observational and numerically simulated data. It turns out that our theoretical results are in pretty good coincidence between the above observational and numerical data. Our theoretical model includes additional distribution of masses, obeying Shechter function (1). It turns out, that the mass distribution (1) does not change our main result (Stephanovich & Godłowski 2015, 2017) that in the stellar systems with multipole (tidal) gravitational interaction, the distribution function of gravitational fields cannot be Gaussian. The crux of the matter here is a long-range character of Newtonian (and derived multipole) interaction between stellar objects. Such character implies that distant objects (like galaxies, their clusters and even dark matter haloes) still "feel each other", which is not the case for Gaussian distribution. The derived non-Gaussian distribution function allows to calculate the distribution of virtually any observables (like angular momentum) of the astronomical structures (not only galaxy clusters but smooth component like halos, which mass dominate the total mass of a cluster, see (Kravtsov, Borgani 2012)) in any (linear or nonlinear) Eulerian approach.

The relation between angular momentum of the galaxy clusters and their masses has also been investigated observationally. It is not difficult to analyze the distribution of the angular momenta for the luminous matter. In real Universe, the luminous galaxies and their structures are surrounded by dark matter halos. These halos are often much more extended and massive than luminous component of the structures. Unfortunately, direct observation of dark matter halos and their angular momenta is

much more complicated. One should not forget, however, that there are observed correlations between luminous and dark matter (sub)structures. It implies the certain dependence between dark matter halos and luminous matter (real galaxies) orientations (Trujillio et al. 2006; Paz et al. 2008; Pereira et al. 2008; Bett et al. 2010; Paz et al. 2011; Kimm et al. 2011; Varela et al. 2012). Recently, the results of Okabe et al. (2018); Codis et al. (2018) based on Horizon-AGN simulation shows the similar dependence. This allows to conclude, that the analysis of angular momentum of luminous matter gives us also the information about angular momentum of the total structure (i.e. that with dark matter halos). As a result, the analysis of the angular momentum of "real" (luminous) galaxies and their structures, is still important as a test for possible structure formation scenario. Note, that investigations of galaxies orientation in clusters are also very important for the analysis of weak gravitational lensing, see Heavens et al. (2000); Heymans et al. (2004); Kiessling et al. (2015); Stephanovich & Godłowski (2015); Codis et al. (2016) for more details.

As generally galaxy clusters do not rotate (Hwang & Lee 2007; Tovmassian 2015), the angular momentum of a cluster is primarily due to spins of member galaxies. Unfortunately, usually we do not know angular momenta of galaxies. So the orientations of galaxies are investigated instead (Oepik (1970); Hawley & Peebles (1975), see Romanowsky & Fall (2012); Pajowska et al. (2019) for present review), as it is assumed that the rotational axes of galaxies are normal to their planes. Such assumption seems to be quite reasonable at least for the spiral galaxies. As a result, stronger alignment of galaxies in a structure means larger angular momentum of the latter.

The question is, if there are any relation between the alignment and mass of the structures. General result of the previous papers is that there is no sufficient evidence for galaxies alignment in less massive structures like groups and poor clusters. However, we observe the alignment of galaxies in rich clusters, see Godłowski (2011); Pajowska et al. (2019) for review. First results (Godłowski, Szydlowski & Flin (2005); Aryal et al (2007)) were qualitative only. Because of that, Godłowski et al. (2010); Godłowski (2012) investigated quantitatively the orientation of galaxies in the sample of 247 rich Abell cluster, using improved Hawley & Peebles (1975) method (see Pajowska et al. (2019) for latest review). In these papers, it was found that the alignment is present in the above sample. Moreover, galaxy orientation increased with numerosness of the cluster. However, the data was not sufficient both to resolve the question about the exact form of this relationship and for confirmation of the hypothesis that the angular momentum of the structure increases with time. This is the reason that we decide to extend our sample and compare observational results with those obtained from simulations.

2. THE FORMALISM

Similar to the papers Stephanovich & Godłowski (2015, 2017) we consider here the quadrupolar (tidal) interaction of the stellar objects

$$\mathcal{H} = -G \sum_{ij} Q_i m_j V(\mathbf{r}_{ij}), \quad V(\mathbf{r}) = \frac{1}{2} \frac{3 \cos^2 \theta - 1}{r^3}, \quad (2)$$

where G is the gravitational constant, Q_i and m_i are, respectively, the quadrupole moment and mass of i -th object, $r_{ij} \equiv |\mathbf{r}_{ij}|$, $\mathbf{r}_{ij} = \mathbf{r}_j - \mathbf{r}_i$ is a relative distance between objects while θ is the apex angle. The Hamiltonian function (2) describes the interaction of quadrupoles, formed both from luminous and dark matter, see [Stephanovich & Godłowski \(2017\)](#) for details.

To account for the mass distribution (1), we begin with the expression for characteristic function $F(\rho)$ of the random gravitational fields' distribution ([Stephanovich & Godłowski 2015, 2017](#)).

$$F(\rho) = \int_V n(\mathbf{r}) \left[1 - \frac{\sin \rho E(\mathbf{r})}{\rho E(\mathbf{r})} \right] d^3r. \quad (3)$$

In the spirit of the article of [Chandrasekhar \(1943\)](#), we rewrite the expression (3) in the form

$$F(\rho) = \int_{V,m} n(\mathbf{r}, m) \left[1 - \frac{\sin \rho E(\mathbf{r}, m)}{\rho E(\mathbf{r}, m)} \right] d^3r dm, \quad (4)$$

where $n(\mathbf{r}, m)$ is the number density (concentration, proportional to probability, see below) of stellar objects (galaxies, their clusters and also dark matter haloes) at the position \mathbf{r} with a mass m . As the average density at large scales can be well regarded as constant (slowly spatially fluctuating to be specific), see [Chandrasekhar \(1943\)](#); [Press & Schechter \(1974\)](#), the number density n in Eq. (4) can be safely considered to be spatially uniform, i.e. $n = n(m)$. In this case the expression (4) reads

$$F(\rho) = \int_{V,m} n(m) \left[1 - \frac{\sin \rho E(\mathbf{r}, m)}{\rho E(\mathbf{r}, m)} \right] d^3r dm, \quad (5)$$

where

$$E(\mathbf{r}, m) = E_0 \frac{3 \cos^2 \theta - 1}{r^4}, \quad E_0 = \frac{1}{2} GQ, \quad Q \approx mR^2 \quad (6)$$

is the quadrupolar field [Stephanovich & Godłowski \(2015\)](#), m is the mass of a stellar object (like galaxy or cluster) and R is its mean radius. We take the function $n(m) \equiv f(m)$ in the form of the Shechter function (1), where m_* and α are adjustable parameters. We obtain the normalization constant A from the condition (see Eq. (4) of [Press & Schechter \(1974\)](#))

$$n = \int_0^\infty n(m) dm, \quad (7)$$

where n is our previous constant concentration [Stephanovich & Godłowski \(2015, 2017\)](#). Note, that there is no problem to take any other dependence $n(m)$ which will not complicate our consideration a lot. As we mentioned above, here we, following [Shechter \(1976\)](#), assume that the luminosity is directly proportional to the first degree of a mass $\tilde{L} \sim m$. But there is no problem to consider the higher degrees in this relation like $\tilde{L} \sim m^k$, $k = 4$. In this case, the argument of the function (1) will be m^k instead of m .

The explicit calculation gives

$$n = A \int_0^\infty \left(\frac{m}{m_*} \right)^\alpha e^{-m/m_*} dm = A m_* \Gamma(1 + \alpha). \Rightarrow A = \frac{n}{m_* \Gamma(1 + \alpha)}. \quad (8)$$

Here $\Gamma(z)$ is Euler Γ - function (Abramowitz & Stegun 1972). Finally we have from (5)

$$F(\rho) = \frac{n}{m_*\Gamma(1+\alpha)} \int_V \int_0^\infty dm \left(\frac{m}{m_*}\right)^\alpha e^{-m/m_*} \left[1 - \frac{\sin \rho E(\mathbf{r}, m)}{\rho E(\mathbf{r}, m)}\right] d^3r, \quad (9)$$

where $E(\mathbf{r}, m)$ is given by the equation (6). It turns out that the equation (8) can be reduced to the Eqs (17) and (18) from Stephanovich & Godłowski (2015) but with slightly renormalized coefficient before $\rho^{3/4}$. This is because under the assumption that n does not depend on coordinates (it depends only on mass, see Eq. (1)), the coordinates and mass turn out to be effectively decoupled. To do so, we perform first the integration over d^3r in (8). This integration is exactly the same as that in Stephanovich & Godłowski (2015) (since the mass enters Eq. (6) through parameter E_0 which is unimportant for coordinate integration) so that we have from (9)

$$F(\rho) = 2\pi \cdot 0.41807255 \rho^{3/4} E_{10}^{3/4} \int_0^\infty m^{3/4} n(m) dm, \quad E_{10} = \frac{1}{2} GR^2. \quad (10)$$

The integral in (10) can be performed as follows

$$\begin{aligned} I &= \int_0^\infty m^{3/4} n(m) dm = \frac{n}{m_*\Gamma(1+\alpha)} \int_0^\infty m^{3/4} \left(\frac{m}{m_*}\right)^\alpha e^{-m/m_*} dm = \\ &= \frac{n m_*^{7/4}}{m_*\Gamma(1+\alpha)} \int_0^\infty x^{\alpha+3/4} e^{-x} dx = n m_*^{3/4} \frac{\Gamma(\alpha + \frac{7}{4})}{\Gamma(\alpha + 1)}. \end{aligned} \quad (11)$$

Finally

$$F(\rho) = 2\pi n m_*^{3/4} \frac{\Gamma(\alpha + \frac{7}{4})}{\Gamma(\alpha + 1)} E_{10}^{3/4} \cdot 0.41807255 \cdot \rho^{3/4} \equiv \kappa \rho^{3/4}, \quad (12)$$

where

$$\kappa = 2\pi n \cdot 0.41807255 \cdot E_0^{*3/4} \frac{\Gamma(\alpha + \frac{7}{4})}{\Gamma(\alpha + 1)}, \quad E_0^* \equiv m_* E_{10} = \frac{1}{2} G m_* R^2 \equiv \frac{1}{2} G Q^*. \quad (13)$$

The expressions (12), (13) give the answer for the case when we have Shechter distribution for galaxies masses. The difference between previous case (Stephanovich & Godłowski (2015, 2017)) of a single mass is that now the width of distribution function of random gravitational fields depends on the fitting parameters m_* and α . Note that for *any* function $n(m)$ the result for characteristic function $F(\rho)$ will be Ex. (12) but with different coefficient κ .

3. CALCULATION OF THE MASS DEPENDENCE OF MEAN ANGULAR MOMENTUM

To derive the mass dependence of mean angular momentum, we should first calculate the distribution function of gravitational fields $f(E)$, then using linear relation between angular momentum L and field E (here, without loss of generality, we consider the moduli of corresponding vectors, see Stephanovich & Godłowski (2015,

2017) for details), derive the distribution function $f(L)$, from which we obtain the desired dependence.

The expression for the field E distribution reads (Stephanovich & Godłowski 2015)

$$f(E) = \frac{1}{(2\pi)^3} \int e^{iE\rho - F(\rho)} d^3\rho \equiv \frac{1}{2\pi^2 E} \int_0^\infty \rho e^{-\kappa\rho^{3/4}} \sin \rho E d\rho, \quad (14)$$

where $F(\rho)$ is the characteristic function (12). Function $f(E)$ is normalized as follows

$$4\pi \int_0^\infty E^2 f(E) dE = 1 \quad (15)$$

and coefficient κ is given by the expression (13). The distribution function of angular momenta can be expressed by usual way from above $f(E)$

$$f(L) = f[E(L)] \left| \frac{dE(L)}{dL} \right|. \quad (16)$$

This gives explicitly (see Stephanovich & Godłowski (2015, 2017))

$$f(\lambda) = \frac{I(\lambda)}{2\pi^2 \lambda^3 \kappa^4 L_0(t)}, \quad (17)$$

where $\lambda = L/(L_0(t)\kappa^{4/3})$,

$$I(\lambda) = \int_0^\infty x \sin x \exp \left[- \left(\frac{x}{\lambda} \right)^{3/4} \right] dx. \quad (18)$$

Function $L_0(t)$ defines the model (CDM or Λ CDM) used by Stephanovich & Godłowski (2017).

3.1. CDM model

Equation (12) shows that the distribution function of angular momenta for the case of distributed masses is similar to that from Stephanovich & Godłowski (2015) with the only change $\alpha \rightarrow \kappa$. This means that the mean dimensionless angular momentum reads (Stephanovich & Godłowski 2015, 2017)

$$\lambda_{max} = 0.602730263. \quad (19)$$

Now we should express parameter κ through galaxy (but not cluster, which is still equals to $M = mN$, where m is galaxy mass, M is cluster mass, N is a number of galaxies in a cluster, see Stephanovich & Godłowski (2015, 2017)) mass m . This quantity is now defined as an average mass with distribution (1)

$$m = \int_0^\infty m_1 n(m_1) dm_1 \equiv \frac{n m_*^2 \Gamma(\alpha + 2)}{m_* \Gamma(1 + \alpha)} = (\alpha + 1) m_* n. \quad (20)$$

The expression (20) implies that the galaxy mass m is related to the mass distribution parameter m_* as

$$m_* = \frac{m}{n(\alpha + 1)}. \quad (21)$$

The next step is to substitute the expression (21) to the expression (13) for κ and express it through galaxy mass m instead of m_* . We have from Ex. (13)

$$\kappa^{4/3} = \frac{mE_{10} n^{1/3}}{\alpha + 1} \left[2\pi \cdot 0.41807255 \cdot \frac{\Gamma(\alpha + \frac{7}{4})}{\Gamma(\alpha + 1)} \right]^{4/3}. \quad (22)$$

In CDM model, the function $L_0(t)$ has the form (Stephanovich & Godłowski 2017)

$$L_0(t) = \frac{2I}{3} \frac{t}{t_0^2}, \quad (23)$$

where $I \approx mR^2$ is a galaxy moment of inertia and t_0 is a time scale. We have from the equation (19) in dimensional units

$$\begin{aligned} L_{max} &= \lambda_{max} L_0 \kappa^{4/3} \equiv 0.6027 \frac{2I}{3} \frac{t}{t_0^2} \frac{mE_{10} n^{1/3}}{1 + \alpha} \left[2\pi \cdot 0.418 \cdot \frac{\Gamma(\alpha + \frac{7}{4})}{\Gamma(\alpha + 1)} \right]^{4/3} \\ &= 0.7281884 \frac{t}{t_0^2} \frac{m^2 n^{1/3}}{1 + \alpha} \zeta^{4/3} GR^4, \quad \zeta = \frac{\Gamma(\alpha + \frac{7}{4})}{\Gamma(\alpha + 1)}. \end{aligned} \quad (24)$$

The comparison of the expression (24) with Ex. (12) from Stephanovich & Godłowski (2015) shows that their only difference is other power of n . Namely, while latter Ex. (12) involves $n^{4/3}$, our expression (24) contains $n^{1/3}$. This is the consequence of the star masses distribution according to the Shechter function. We note also that the above mass distribution leaves the power of galaxy mass m intact, i.e. both expressions involve m^2 . This gives that in the first scenario (see below and Eq. (13) of Stephanovich & Godłowski (2017)) the dependence of L_{max} on galaxy cluster mass $M = mN$ will be the same $\sim M^{5/3}$. At the same time, in the second scenario (Eq. (15) of Ref. Stephanovich & Godłowski (2017)) the dependence on M will be $M^{1/3}$ instead of $M^{4/3}$. We now derive the dependencies on M within both scenarios of Ref. Stephanovich & Godłowski (2017).

3.1.1. First scenario

In this scenario we represent galaxy volume as $V = R^3$ (Stephanovich & Godłowski 2017), where R is the mean radius of a galaxy. In this case we have from (24)

$$\begin{aligned} L_{max} &= \eta m^2 n^{1/3} R^4 = \eta m^2 R^4 \frac{N^{1/3}}{V^{1/3}} \equiv \eta m^2 R^4 \frac{N^{1/3}}{R} = \eta m^2 R^3 N^{1/3} = \\ &= \eta \frac{R^3}{N} M^{5/3} \frac{m^{1/3}}{N^{1/3}} = \eta \frac{1}{n} M^{5/3} \frac{\rho^{1/3}}{n^{1/3}} = \eta M^{5/3} \frac{\rho^{1/3}}{n^{4/3}}, \quad \eta = \frac{t}{t_0^2} \frac{0.728G}{1 + \alpha} \zeta^{4/3}, \\ \rho &= \frac{m}{V}, \quad n = \frac{N}{V}. \end{aligned} \quad (25)$$

The comparison of Eq. (25) and Eq. (13) from Ref. Stephanovich & Godłowski (2017) shows that the $M^{5/3}$ is the same, but the galaxies concentration n now enters in the power 4/3 instead of 1/3. One more difference is that now Shechter exponent α (see Eq. (1)) enters the answer via parameters η and ζ . It should be extracted from the best fit between expression (25) and data, taken either from observations or numerical simulations.

3.1.2. Second scenario

In this scenario the galaxy volume is $V = R_A^3$, where R_A is a mean galaxy cluster radius. We have from (24)

$$\begin{aligned} L_{max} &= \eta m^2 n^{1/3} R^4 = \eta m^2 R^4 \frac{N^{1/3}}{R_A} = \eta \frac{R}{R_A} R^3 m^2 N^{1/3} = \\ &= \eta \frac{R}{R_A} R^3 m^2 \frac{M^{1/3}}{m^{1/3}} = \eta \frac{R}{R_A} R^3 m^{5/3} M^{1/3}. \end{aligned} \quad (26)$$

It is seen, that contrary to Eq. (15) of Ref. [Stephanovich & Godłowski \(2017\)](#), here we have $M^{1/3}$. Also, the Shechter parameter α enters the answer.

3.2. Λ CDM model

Here, similar to [Stephanovich & Godłowski \(2015\)](#), we should isolate the contribution from time dependent functions $f_{1,2}(\tau)$ ($\tau = t/t_0$, $t_0 = 2/(3H_0\sqrt{\Omega_\Lambda})$, see Ex. (46) of [Stephanovich & Godłowski \(2015\)](#) and $i = 1, 2$ numbers the orders (first and second respectively) of perturbation theory. Following [Stephanovich & Godłowski \(2015\)](#), we have for argument of the distribution function $H(\lambda, t)$ (Eq. (44) of [Stephanovich & Godłowski \(2015\)](#))

$$\lambda(\tau) = \frac{L}{I\kappa^{4/3}} \frac{1}{f_i(\tau)}. \quad (27)$$

Similar to above CDM model, the maximum of the distribution function $\lambda_{max} = 0.602730263$ generates following relation

$$\begin{aligned} L_{max} &= I\kappa^{4/3} \cdot 0.6027 f_i(\tau) \equiv \eta_{\Lambda CDM i}(\tau) m^2 R^4 n^{1/3}, \\ \eta_{\Lambda CDM i}(\tau) &= f_i(\tau) \frac{0.6027 \Psi^{4/3} G}{2(\alpha + 1)}, \quad \Psi = 2\pi \cdot 0.418 \cdot \frac{\Gamma(\alpha + \frac{7}{4})}{\Gamma(\alpha + 1)}. \end{aligned} \quad (28)$$

The relation (28) is almost similar both in CDM and Λ CDM models. The only difference is in the functions $f_i(\tau)$, where in CDM model

$$f_1(\tau) = (2/3)\tau, \quad f_2(\tau) = (-4/3)\tau^{1/3}. \quad (29)$$

It is seen that the substitution of functions $f_{1,2}$ (29) yields immediately the expressions (25) and (26) for CDM model. In Λ CDM model the functions $f_{1,2}(\tau)$ should be taken from the solution of the differential equations (30) and (31) of [Stephanovich & Godłowski \(2015\)](#).

As the expression (28) for L_{max} is formally equivalent to Eqs (25) and (26), the dependences $L_{max}(M)$ are the same as those defined by Eqs (25) and (26) except that we should use now $\eta_{\Lambda CDM i}(\tau)$.

The representative plots of the function $H(\lambda, \tau) = 2I(\lambda, \tau)/(\pi\lambda)$ ([Stephanovich & Godłowski 2015](#)) and the maximal value $\lambda_{max}(\tau)$ for the mass-dependent density (1) are reported in Fig. 1. Left and middle panels show the results for the first (Eq. (30) of [Stephanovich & Godłowski \(2015\)](#)) and second orders (Eq. (31) of Ref. [Stephanovich & Godłowski \(2015\)](#)) of perturbation theory. First, it is seen,

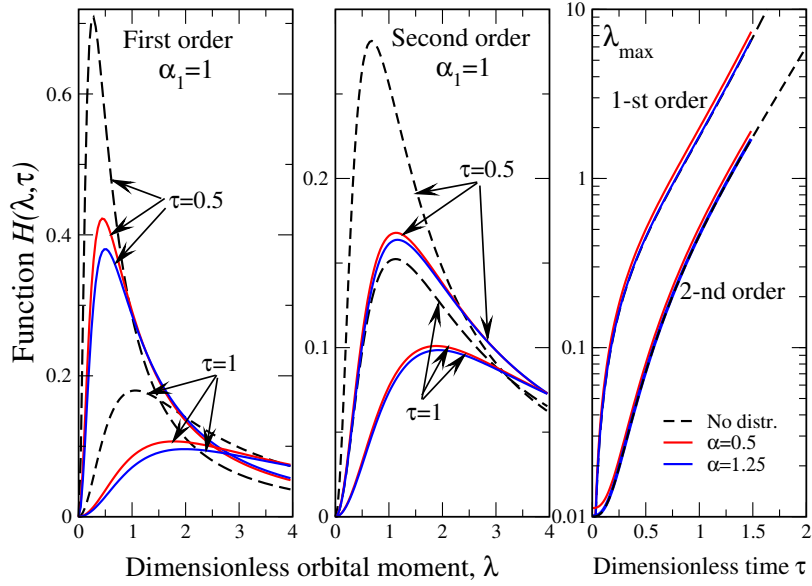


Fig. 1. Time evolution of the distribution function $H(\lambda, \tau)$ in Λ CDM model for the case of mass-dependent density (1). Left panel: first order of perturbation theory. Middle panel: second order. Right panel shows the dependence $\lambda_{max}(\tau)$ in the first and second orders of perturbation theory. In all panels, dashed lines (marked as "No distr." in the right panel) correspond to the previous case of mass-independent density n . We consider two Shechter exponents $\alpha = 0.5$ (red curves) and 1.25 (blue curves), coded by colors and explained in the legend in right panel. Parameter of Λ CDM model $\alpha_1 = \left(\frac{1-\Omega_\Lambda}{\Omega_\Lambda}\right)^{1/3} = 1$.

that the distribution of masses does not make qualitative difference in the shape of distribution function. Namely, the shape of the dashed black curves (those without masses distribution) and red and blue ones is the same. At the same time, the distribution functions $H(\lambda, \tau)$ has substantially smaller amplitudes in the case of mass distribution. This means that the presence of mass distribution changes the functions $H(\lambda, \tau)$ quantitatively. The influence of Shechter exponent α (Press & Shechter 1974; Shechter 1976) is minimal - the curves $H(\lambda, \tau)$ as well as $\lambda_{max}(\tau)$ (right panel) are almost the same for $\alpha = 1.25$ and 0.5 , which is a big difference. This means that while the distribution of masses by itself changes the distribution function quantitatively, the value of constant α in that distribution is of minute influence. Our analysis shows that the above tendency persists for any time instant (in Fig. 1 we have only two time instants $\tau = 0.5$ and 1) and any reasonable $\alpha > 0$. The maximal values λ_{max} are almost independent of the presence of mass distribution. Really, it is seen from right panel of Fig. 1, that both curves for no mass distribution (black dashed lines) and those with it lie very close to each other. This means simply that the physics of the system under consideration is determined by the distribution of random gravitational fields, than that of masses of stellar objects. Maybe the "complete" dependence $n(\mathbf{r}, m)$ (4) (rather than present simplified situation $n(m)$ in each spatial point \mathbf{r} (5)) will improve the situation. On the other hand, it is well acceptable that the robust distribution of gravitational fields is simply not susceptible to the small corrections like mass distribution. Latter, in turn, may mean, that next important step in the physics of galaxies formation is to consider the short-range interaction between galaxies (due to dark matter presence, for instance) so that the real average angular momentum (and not the distribution function maximum, considered so far) will appear, see Eq. (48) of Ref. Stephanovich & Godłowski (2015) and Eq. (28) of Ref. Stephanovich & Godłowski (2017).

4. OBSERVATIONAL DATA

First part of our data is the sample of rich Abell clusters containing at least 100 member galaxies each (Pajowska et al. 2019). The sample contains 247 clusters and it was selected on the base of the PF catalogue (Panko & Flin (2006)), see Pajowska et al. (2019) for details). However in the present paper we decide to restrict ourselves to 187 clusters which have explicit redshifts. As our PF cluster sample was not sufficient to confirm hypothesis that galaxies alignment decreases with redshift, we decide to enlarge our sample on the DSS base.

From ACO Catalogue (Abell, Corwin & Olowin 1989) we selected all Abell clusters with galactic latitude $b > 40^\circ$ and richness class ≥ 1 . This gives us 1238 structures of galaxies from which we selected only those with redshifts $z < 0.2$ (Struble & Rood 1999). Therefore, 377 clusters have been left for analysis. From DSS we extracted the area covering $2\text{Mpc} \times 2\text{Mpc}$ ($h = 0.75$, $q_0 = 0.5$) around each cluster. We applied the FOCAS package (Jarvis & Tyson 1981) to the extracted regions and obtained catalogues of galaxies, considering objects within the magnitude range $(m_3, m_3 + 3)$, where m_3 is the magnitude of the third brightest galaxy. The catalogues obtained automatically were visually corrected in order to

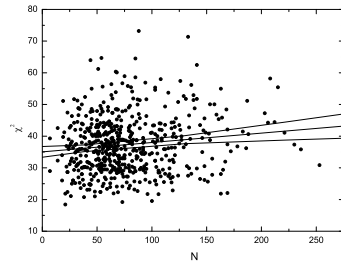
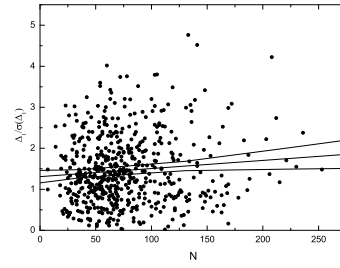
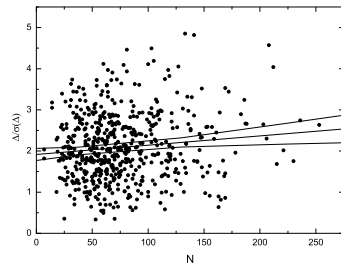
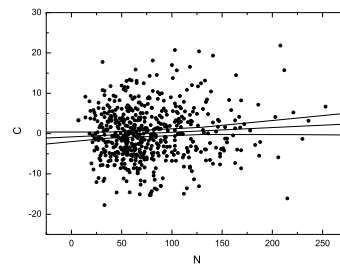
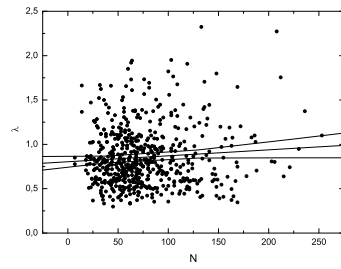
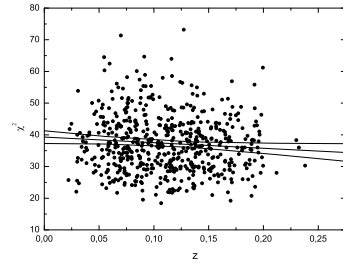
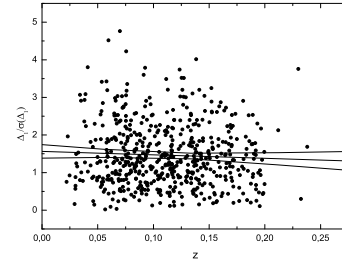
(a) Relation between N and χ^2 (b) Relation between N and $\Delta_1/\sigma(\Delta_1)$ (c) Relation between N and $\Delta/\sigma(\Delta)$ (d) Relation between N and C (e) Relation between N and λ

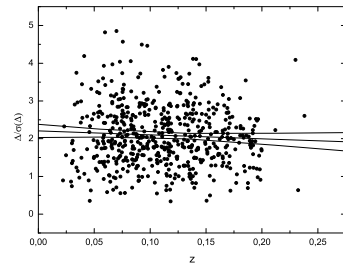
Fig. 2. The dependence of the number N of galaxies in a cluster on different statistical parameters of the Sample B. The bound errors, at the confidence level 95%, were presented as well.



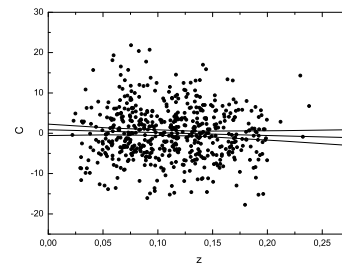
(a) Relation between redshift z and χ^2



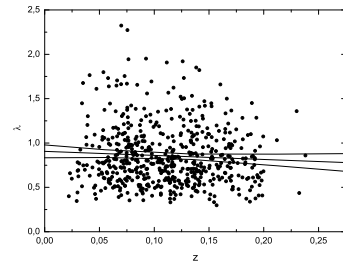
(b) Relation between redshift z and $\Delta_1/\sigma(\Delta_1)$



(c) Relation between redshift z and $\Delta/\sigma(\Delta)$



(d) Relation between redshift z and C



(e) Relation between redshift z and λ

Fig. 3. The dependence of cluster redshift z on different statistical parameters of the Sample B. The bound errors, at the confidence level 95%, were presented as well.

reduce the possible incorrect star/galaxy classification. FOCAS calculates the catalogue parameters using the moments of pixel distribution in an object. There are three steps from the basic image to the object list in FOCAS: segmentation, area assembly and object evaluation. The various parameters characterizing the individual images in the segmented areas were calculated. In FOCAS, the object location is defined by centroids:

$$\bar{x} = \frac{1}{M_{00}} \sum_A x_i [I(x, y) - I_s]. \quad (30)$$

$$\bar{y} = \frac{1}{M_{00}} \sum_A y_i [I(x, y) - I_s], \quad (31)$$

where M_{00} is zero moment, which is equal to:

$$M_{00} = \sum_A [I(x, y) - I_s]. \quad (32)$$

The summation over A means that the sum includes all pixels in the object-defining area A . $I(x, y)$ is the intensity corresponding to the density at the location (x, y) in the digital plate image. I_s is the intensity corresponding to the average plate density at the object location. Shape information about the object is obtained from the higher central moments:

$$M_{ij} = \sum A (x - \bar{x})^i (y - \bar{y})^j [I(x, y) - I_s]. \quad (33)$$

The object position angle is calculated using above central moments:

$$\tan(2\theta) = \frac{2M_{11}}{M_{20} - M_{02}}. \quad (34)$$

Galaxy ellipticity reads

$$e = 1 - \frac{\lambda_2}{\lambda_1}, \quad (35)$$

where

$$\begin{aligned} \lambda_1^2 &= \frac{1}{2} \left((M_{20} + M_{02}) + \sqrt{(M_{20} - M_{02})^2 + 4M_{11}^2} \right), \\ \lambda_2^2 &= \frac{1}{2} \left((M_{20} + M_{02}) - \sqrt{(M_{20} - M_{02})^2 + 4M_{11}^2} \right). \end{aligned} \quad (36)$$

Each catalogue contains information about the right ascension and declination of each galaxy, its coordinates x and y on the photographic plate, instrumental magnitude, object area, galaxy ellipticity and the position angle of the major axis of galaxy image. The equatorial galaxy coordinates for the epoch 2000 were computed according to the rectangular coordinates of DSS scans. We calculate the position angle and ellipticity of each galaxy cluster using the method described by [Carter & Metcalfe \(1980\)](#) which is also based on the first five moments of the observed distribution of galaxy coordinates x_i, y_i .

5. STATISTICAL STUDIES

Hawley & Peebles (1975) propose to analyze the distribution of galaxies angular momenta by that of the observed position angles of the galactic image major axes. The direction of the angular momentum is then believed to be perpendicular to that of the major galaxy axis. This means that in the original version of the method the face-on and nearly face-on galaxies must be excluded from the analysis. This method can also be extended for the studies of the spatial orientation of galaxy planes (Flin & Godłowski 1986).

The idea of Hawley & Peebles (1975) is to use the statistical tests for investigation of the position angles distribution. The higher value of statistics means greater deviation from isotropic distribution i.e. stronger alignment of galaxies angular momenta in the analyzed structures. Since Hawley & Peebles (1975) paper this method has become the standard tool for searching of galactic alignments. Recent improvement and revision of this method was presented in Pajowska et al. (2019).

In the present paper we follow the analysis from Stephanovich & Godłowski (2017). The entire range of investigated angles was divided into n bins. As the aim of the method is to detect non-random effect in the galaxies orientation, we first check if considered distribution deviates from isotropic one. Following Stephanovich & Godłowski (2017), in the present paper we use χ^2 and Fourier tests. We also extend our analysis for first auto-correlation and Kolmogorov-Smirnov (K-S) tests (Hawley & Peebles (1975); Flin & Godłowski (1986); Godłowski et al. (2010); Godłowski (2012) see Pajowska et al. (2019) for last review).

The statistics χ^2 is:

$$\chi^2 = \sum_{k=1}^n \frac{(N_k - N p_k)^2}{N p_k} = \sum_{k=1}^n \frac{(N_k - N_{0,k})^2}{N_{0,k}}, \quad (37)$$

where p_k are probabilities that chosen galaxy falls into k -th bin, N is the total number of galaxies in a sample (in a cluster in our case), N_k is the number of galaxies within the k -th angular bin and $N_{0,k} = N p_k$ is the expected number of galaxies in the k -th bin. Note that the number of degrees of freedom of the χ^2 test is $n - 1$, mean value $E(\chi^2) = n - 1$ while the variance $\sigma^2(\chi^2) = 2(n - 1)$. As in our analysis $n = 36$, we obtain the values $E(\chi^2) = 35$ while $\sigma^2(\chi^2) = 70$, i.e. $\sigma(\chi^2) = 8.367$.

The first auto-correlation test quantifies the correlations between galaxy numbers in neighboring angle bins. The statistics C reads

$$C = \sum_{k=1}^n \frac{(N_k - N_{0,k})(N_{k+1} - N_{0,k+1})}{[N_{0,k}N_{0,k+1}]^{1/2}}, \quad (38)$$

where $N_{n+1} = N_1$. When, as in present paper, we analyze the distribution of the position angles, than all $N_{k,0} = N p_k$ are equal to each other and $E(C) = -1$ while $D(C) \approx n$ (i.e. $\sigma(C) \approx \sqrt{n} = 6$), see Godłowski (2012); Pajowska et al. (2019) for details.

If we assume that deviation from isotropy is a slowly varying function, we can use the Fourier test:

$$N_k = N_{0,k}(1 + \Delta_{11} \cos 2\theta_k + \Delta_{21} \sin 2\theta_k + \Delta_{12} \cos 4\theta_k + \Delta_{22} \sin 4\theta_k + \dots). \quad (39)$$

In this test, the statistically important are the amplitudes

$$\Delta_1 = (\Delta_{11}^2 + \Delta_{21}^2)^{1/2}, \quad (40)$$

(only the first Fourier mode is taken into account) or

$$\Delta = (\Delta_{11}^2 + \Delta_{21}^2 + \Delta_{12}^2 + \Delta_{22}^2)^{1/2}, \quad (41)$$

where the first and second Fourier modes are analyzed together. We investigate the statistics $\Delta_1/\sigma(\Delta_1) = (\Delta_{11}^2/\sigma^2(\Delta_{11}) + \Delta_{21}^2/\sigma^2(\Delta_{21}))^{1/2}$ and $\Delta/\sigma(\Delta) = (\Delta_{11}^2/\sigma^2(\Delta_{11}) + \Delta_{21}^2/\sigma^2(\Delta_{21}) + \Delta_{12}^2/\sigma^2(\Delta_{12}) + \Delta_{22}^2/\sigma^2(\Delta_{22}))^{1/2}$ (see [Godłowski et al. \(2010\)](#); [Godłowski \(2012\)](#); [Pajowska et al. \(2019\)](#) for details). Note that the expression $\frac{\Delta_j^2}{\sigma^2(\Delta_j)}$ means that elements of Δ^2 should be divided by their errors rather than that the total factor Δ_j^2 is divided by its error. Namely, the expectation values of the total factors are $E\left(\frac{\Delta_1}{\sigma(\Delta_1)}\right) = 1.2247$ and $E\left(\frac{\Delta}{\sigma(\Delta)}\right) = 1.8708$ while $\sigma^2(\Delta_1/\sigma(\Delta_1)) = 1/2$, and $\sigma^2(\Delta/\sigma(\Delta)) = 1/2$ (i.e. errors of the total factors equal to $\sqrt{2}$) - see [Godłowski \(2012\)](#); [Pajowska et al. \(2019\)](#) for details.

In the case of K-S test, the statistics under study is λ :

$$\lambda = \sqrt{N} D_n \quad (42)$$

which is given by limiting Kolmogorov distribution, where

$$D_n = \sup |F(x) - S(x)| \quad (43)$$

and $F(x)$ and $S(x)$ are theoretical and observational distributions of the investigated angle respectively. [Wang et al. \(2003\)](#) analyzing the limiting form of D_n function found that $\mu(\lambda) = 0.868731$ while $\sigma^2(\lambda) = 0.067773$ i.e $\sigma(\lambda) = 0.260333$ (see also [Pajowska et al. \(2019\)](#) for discussion).

Using extended [Hawley & Peebles \(1975\)](#) method it is possible to analyze both the alignment dependence on particular parameter like richness of galaxy cluster [Godłowski et al. \(2010\)](#) and quantitatively answer the question if an alignment is present in a sample (see [Pajowska et al. \(2019\)](#) for last revision). In our previous papers [Godłowski et al. \(2010\)](#); [Stephanovich & Godłowski \(2017\)](#), using sample of 247 PF rich Abell clusters, it was shown that alignment of galaxies in a cluster increases significantly with its richness. Unfortunately available data was insufficient for persuasive conclusion about correctness of theoretically predicted by [Stephanovich & Godłowski \(2015, 2017\)](#) dependence of analyzed statistics on redshift z .

For this reason we perform the investigations of our samples of galaxy clusters checking if there is a significant dependence between analyzed statistics and both richness and redshifts of the clusters. As a first step we analyzed the linear model $Y = aX + b$. The Y are the values of analyzed statistics i.e. χ^2 , $\Delta_1/\sigma(\Delta_1)$, $\Delta/\sigma(\Delta)$, C and λ (see [Stephanovich & Godłowski \(2017\)](#) for details) while X is the number of analyzed galaxies in each particular cluster or its redshift z respectively. Our null hypothesis H_0 is that analyzed statistics Y does not depend on X . This means that we should analyze the statistics $t = a/\sigma(a)$, which has Student's

distribution with $u - 2$ degrees of freedom, where u is the number of analyzed clusters. In other words, we test H_0 hypothesis that $t < 0$ against H_1 hypothesis that $t > 0$, where $t > 0$ corresponds to the case of dependence on number of member galaxies in clusters and $t < 0$ to the case of dependence on redshift z . In order to reject the H_0 hypothesis, the value of observed statistics t should be greater than t_{cr} which could be obtained from the tables. For example, for sample of 247 clusters analyzed in [Stephanovich & Godłowski \(2017\)](#) (our sample A) at the significance level $\alpha = 0.05$, the value $t_{cr} = 1.651$. For our sample B (564 clusters) at the significance level $\alpha = 0.05$, the value $t_{cr} = 1.648$.

The results of our analysis are presented in the table 1 and figs 2,3. One could discern from the table 1, that if the analysis of the sample A confirms the alignment increasing with cluster richness, then any test confirm negative deviation of linear regression parameter from zero in the case of alignment dependence on redshift. However, both above dependencies can be confirmed from the full sample (564 clusters) analysis. At first we analyzed statistics i.e. alignment, which increases significantly with richness of a cluster, confirming the result obtained in [Godłowski et al. \(2010\)](#); [Stephanovich & Godłowski \(2017\)](#) as well as theoretical prediction [Stephanovich & Godłowski \(2015\)](#). The details are also presented in the figures 2(a) - 2(e). Moreover, we could conclude that alignment decreases with z , which means that it increases with time as predicted by [Stephanovich & Godłowski \(2015, 2017\)](#); [Schmitz et al. \(2018\)](#) (see figures 3(a) - 3(e)).

However, closer look at the results show that situation is not so clear yet. This is because in real data the cluster richness usually decreases also with the redshift z . Quantitatively, in linear model, the dependence between richness and redshift of a cluster is $N(z) = az + b$. In this model, we obtain the value of t statistics $t = -7.066$. This is the reason that we repeated our analysis as 3D model $Y = a_1N + a_2z + b$. Note, that until now, such 3D analysis has not been performed in galaxies alignment studies, but due to the above reason, we consider it to be necessary here. In this extended analysis, the test statistics t are given by formulae $t_1 = a_1/\sigma(a_1)$ and $t_2 = a_2/\sigma(a_2)$. From Table 2, we could confirm that alignment increases significantly with cluster richness. One should note that all our tests show that statistics are decreasing with z , however values of t statistics are too small to make statistically significant (significance level $\alpha = 0.05$) effect.

6. SIMULATIONS

The [Illustris Project \(2018\)](#) was the simulation base for our present study. The Project uses the AREPO code for hydrodynamic realizations of a $(106.5Mpc)^3$ cosmological volume ([Springel 2010](#)). The simulation assumes a Λ CDM cosmology with the $\Omega_m = 0.2726$, $\Omega_\Lambda = 0.7274$, $\Omega_b = 0.0456$, $\sigma_8 = 0.809$, $n_s = 0.963$, and $H_0 = 100 \cdot h \cdot km \cdot s^{-1}Mpc^{-1}$ with $h = 0.704$. It contains multiple resolution runs with the highest resolution performed for Illustris - 1. Three different physical configurations have been applied: dark matter only as well as non-radiative and full galaxy formation. In the first case (dark matter only), the mass was treated as collisionless in the simulations. The non-radiation configuration also adds gas hydrodynamics, but ignores radiative cooling and star formation processes. The full

TABLE 1

THE STATISTICS $T = A/\sigma(A)$ FOR OUR SAMPLE OF ABELL CLUSTERS. SAMPLE A - 247 RICH ABELL CLUSTERS FROM PF CATALOGUE (AS IN STEPHANOVICH & GODŁOWSKI (2017)). SAMPLE B - FULL SAMPLE OF 564 CLUSTERS (DIRECTLY KNOWN REDSHIFT)

Test	$S = f(N)$	$S = f(z)$
Sample A		
χ^2	1.872	-0.769
$\Delta_1/\sigma(\Delta_1)$	1.613	0.611
$\Delta/\sigma(\Delta)$	1.964	-0.066
C	1.352	1.343
λ	2.366	0.176
Sample B		
χ^2	3.402	-2.342
$\Delta_1/\sigma(\Delta_1)$	2.857	-1.452
$\Delta/\sigma(\Delta)$	3.142	-1.646
C	1.825	-1.305
λ	2.333	-1.953

galaxy formation physics contains (in addition to the previously mentioned ones) also processes related to galaxy emergence through a model described in [Vogelsberger et al. \(2013\)](#). Illustris-1 consists of 136 runs for different redshifts z where the initial conditions was generated at $z = 127$ for snapshot 0 and evolved to $z = 0$ for snapshot 135.

Illustris successfully follows the coevolution of dark and visible matter. Haloes, subhaloes, and their basic properties have been identified with the FOF and SUBFIND algorithms ([Davis et al. 1985](#); [Springel et al. 2001](#); [Dolag et al. 2009](#)), at every of the 136 stored snapshots. We have added information from the supplementary catalog to the resulting directory of Haloes from [Zjupa & Springel \(2017\)](#). The code was written in such a manner that it can run both as a postprocessing option to increase existing catalogues or as part of the regular group finding.

From Illustris-1 we select Haloes at $z = 0$. We obtained 119 Haloes with total mass exceeding $10^{13}M_{\odot}$ and 1435 ones with total mass higher than $10^{12}M_{\odot}$. The angular momentum parameter for extracted Haloes was taken from [Zjupa & Springel \(2017\)](#).

Illustris simulations give direct value of both mass of the structures and their angular momentum. Present available data from Ilustris are evolved to $z = 0$, so it is possible to study the dependence of angular momentum as the function of cluster mass but unfortunately not of redshift. However as we know directly the cluster angular momentum, it is not necessary to assume the linear relation between angular momentum and mass. Since theoretical modeling predicts usually the power law re-

TABLE 2

THE STATISTICS $T = A/\sigma(A)$ FOR 3D ANALYSIS OF OUR SAMPLE OF ABELL CLUSTERS. SAMPLE B - FULL SAMPLE OF 564 CLUSTERS (DIRECTLY KNOWN REDSHIFT)

Test	$S = f(N)$	$S = f(z)$
Sample B		
χ^2	2.846	-1.434
$\Delta_1/\sigma(\Delta_1)$	2.250	-0.718
$\Delta/\sigma(\Delta)$	2.625	-0.811
C	1.538	-0.814
λ	2.000	-1.302

TABLE 3

THE ILUSTRIS RELATION BETWEEN ANGULAR MOMENTUM AND MASS SIMULATIONS

Mass	a	$\sigma(a)$	$t = a/\sigma(a)$
$> 10^{12}$	1.807	0.028	66.93
$> 10^{13}$	1.708	0.114	14.94

lations (see also [Stephanovich & Godłowski \(2015\)](#) for review) we could study the model $J = b \cdot M^a$. The latter relation could easily be rendered as a linear model $\ln J = \ln b + a \ln M$.

The results of the analysis are presented in the table 3 and figure 4. Analysis of Ilustris Simulation confirms that angular momentum of a cluster increases with its mass. In this case, the coefficient $a = 1.807 \pm 0.028$ (fig. 4(a)) The analysis of a sample, where only the most massive clusters (mass $M > 10^{13}$ solar mass) are left, gives $a = 1.708 \pm 0.114$ (fig. 4(b)) which is close to most popular theoretical prediction $a = 5/3 \approx 1.667$ (see [Godłowski et al. \(2010\)](#); [Stephanovich & Godłowski \(2015, 2017\)](#) for details).

7. OUTLOOK

In the present paper we have shown that the distribution of masses of the stellar objects does not alter substantially the distribution function of their gravitational fields. This shows that the main contribution to latter distribution function comes from the long-range Newtonian interaction between astronomical objects rather than from the distribution of their masses. At the same time, the mass distribution alters the dependence of L_{max} on astronomical objects concentration n (see Eq. (25)) and total cluster mass M (see Eq. (26)), which is observationally important. To discern, which of the dependencies (25) or (26) is realized in practice, the additional observational data is needed. As total interaction potential contains both luminous and

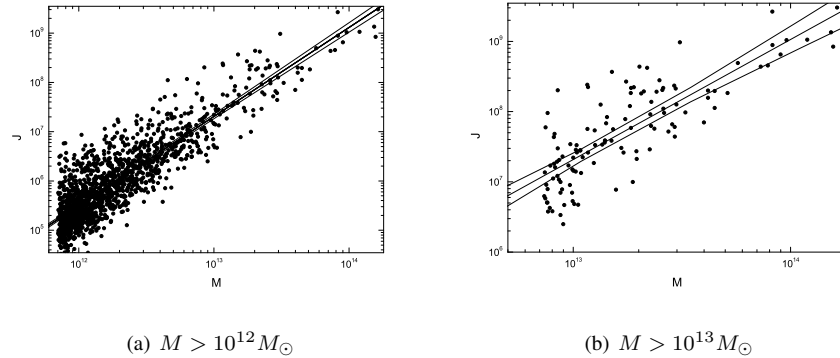


Fig. 4. Relation between angular momentum and mass of a cluster derived from Illustris simulation for different total masses M . The bound errors, at the confidence level 95%, were presented as well.

dark matter components, one can ask a question about alignment of sub-dominant galaxies, even though the majority of galaxy clusters angular momenta is related to the smooth dark matter halo component. This question becomes important in view of the fact that mass distribution (1) alters the dependence on total cluster mass M (26). Namely, in the halo model (Schneider & Bridle 2010), where the galaxies are embedded in a dark matter halo, latter may mediate the intergalactic interaction, adding possible short-range terms to it. That is to say, to "see each other" in a dark matter halo, the galaxies should go closer than in an empty space.

Note, that the observational results about lack of alignment of galaxies for less clumpy (so called poor) clusters, as well as evidence for such alignment in the clumpy (rich) ones (Godłowski, Szydlowski & Flin (2005); Aryal et al (2007), see also Godłowski (2011) for incremental study and relevant references) clearly shows that angular momentum of galaxy groups and clusters increases with their mass (richness). The generalized analysis, based on Eq. (4), where $n = n(r, m)$ (i.e. the mass becomes spatially distributed), will improve the overall understanding, which can additionally be tested against observed galaxy shape distributions and alignments. The problem of angular momenta alignment due to their interactions as well as those with dark matter haloes has been simulated by Hahn et al. (2007). The main effect there is the presence of a threshold cluster mass (richness) value. Latter is related to mutual alignment of clusters and dark matter haloes axes. This fact can be analyzed on the base of more general model (4), which accounts for spatially inhomogeneous distribution of number density of stellar objects as well as for its mass dependence. We postpone the consideration of this interesting question for the future publications.

Our formalism permits studying this effect (see Stephanovich & Godłowski (2017)) as well as the nonequilibrium time evolution of luminous astronomical objects (with respect to dark matter haloes) within the Λ CDM model. The combination of stochastic dynamical approaches (Garbaczewski & Stephanovich 2009, 2011) along with deterministic one defined in Λ CDM model, may permit to answer (at

least qualitatively) the question about the galaxies (and their clusters) initial alignment at the time of their formation. The questions about how dark matter haloes influence (mediate) latter alignment, can also be answered within the above dynamic approach.

Our statistical analysis of Abell clusters sample shows that alignment of galaxies and their clusters angular momenta increases substantially with cluster mass. This result is confirmed also by 3D analysis, consisting in the studies of the dependence of galaxies alignment in a cluster both on its richness and redshift. We have also found that alignment decreases with redshift i.e. increases with time, but above 3D studies show that this effect is too faint to be confirmed statistically at the significance level $\alpha = 0.05$. Probable reason is that the corresponding relaxation time is too long. So for future investigations more extended data containing larger number of galaxy clusters (and with higher redshifts) are required. The comparison of our theoretical results with those of the Illustris simulation also confirms the increase of galaxies angular momenta with cluster mass. Moreover, latter comparison confirms the power law relation with coefficient, very close to $5/3$, which is the value favored by most popular theoretical predictions - see, for instance, [Stephanovich & Godłowski \(2015, 2017\)](#). This may point that the approach of [Stephanovich & Godłowski \(2015, 2017\)](#) correctly reflects main features of galaxies and their clusters formation.

Let us finally note, that as we have shown above, our results are in close conformity with commonly preferred model of the galaxies formation, i.e. so-called hierarchic clustering model ([Peebles 1969](#)), improved recently by taking into account tidal torque scenario.

REFERENCES

- Abell, G., Corwin, H., Olowin, R., 1989, *AJSS*, 70, 1
- Abramowitz, M., Stegun, I., 1972, *Handbook of Mathematical Functions with Formulas, Graphs, and Mathematical Tables* (New York: Dover).
- Aryal, B., Paudel, S., Saurer, W., 2007, *MNRAS*, 379, 1011
- Bartolo, N., Komatsu, E., Matarrese, S., Riotto, A., 2004, *Phys. Rep.* 402, 103
- Bett, P., Eke, V., Frenk, C. S., Jenkins, A., Okamoto, T. 2010, *MNRAS*, 404, 1137
- Carter D., Metcalfe N., 1980, *MNRAS*, 191, 325
- Catelan, P., Theuns, T., 1996, *MNRAS*, 282, 436
- Catelan, P., Theuns, T., 1996, *MNRAS*, 282, 455
- Chandrasekhar, S., 1943, *Rev. Mod. Phys.*, 15, 1
- Codis, S., Dubois, Y., Pichon, C., Devriendt, J., Slyz, A., 2016, in *The Zeldovich Universe: Genesis and Growth of the Cosmic Web*, eds. Rien van de Weygaert, Sergei Shandarin, Enn Saar, Jaan Einasto, *Proceedings of the International Astronomical Union, IAU Symposium*, Volume 308, p. 437
- Codis, S.; Jindal, A.; Chisari, N. E.; Vibert, D.; Dubois, Y.; Pichon, C.; Devriendt, J. 2018 *MNRAS*, 481, 4753
- Davis M., Efstathiou G., Frenk C. S., White S. D. M., 1985, *ApJ*, 292, 371
- Dekel, A. 1985, *ApJ*, 298, 46
- Dolag, K., Borgani, S., Murante, G., Springel, V. 2009, *MNRAS*, 399, 497
- Doroshkevich, A. G. 1970, *Astrofizika*, 6, 581
- Doroshkevich, A. G. 1973, *ApJ*, 14, 11

- Efstathiou, G. A., Silk, J., 1983, The Formation of Galaxies, *Fundamentals of Cosm. Phys.* 9, 1
- Flin, P., Godłowski, W. 1986, *MNRAS*, 222, 525
- Garbaczewski, P., Stephanovich, V. A., 2009, *Phys. Rev. E*, 80, 031113
- Garbaczewski, P., Stephanovich, V. A., 2011, *Phys. Rev. E*, 84, 011142
- Giahi-Saravani, A., Schäfer, B.M. 2013 *MNRAS*, 437, 1847
- Godłowski, W., Szydlowski, M., Flin, P. 2005, *Gen. Rel. Grav.* 37, (3) 615
- Godłowski, W., 2011, *IJMPD*, 20, 1643
- Godłowski, W., 2012, *ApJ*, 747, 7
- Godłowski, W., Piwowarska, P., Panko, E., Flin, P., 2010, *ApJ*, 723, 985
- Hahn, O., Carollo, C.M., Porciani, C., Dekel, A., 2007, *MNRAS*, 381, 41
- Heavens, A., Refregier A., Heymans, C., 2000, *MNRAS*, 232, 339.
- Hawley, D. I., Peebles P. J. E., 1975, *AJ*, 80, 477
- Heymans, C., et al., 2004, *MNRAS*, 347, 895
- Hwang, H. S., Lee M. G., 2007, *ApJ*, 662, 236
- Illustris Project <http://www.illustris-project.org>
- Jarvis, J., Tyson, J., 1981, *AJ* 86, 476
- Joachimi, B., et al. 2015, *Space Science Reviews* 193, 1
- Kiessling, A., Cacciato, M., Joachimi, B., Kirk, D., Kitching, T. D., Leonard, A., Mandelbaum, R., Schaefer, B. M., et al., 2015, *Space Science Reviews* 193, 67
- Kimm, T., Devriendt, J., Slyz, A., Pichon, C., Kassin, S. A., Dubois, Y. 2011, *astro-ph/1106.0538*
- Kravtsov, A.V., Borgani, S., 2012, *ARA&A*, 50, 353
- Lee, J., Pen, U., 2000, *ApJ*, 532, L5
- Lee, J., Pen, U., 2001, *ApJ*, 555, 106
- Lee, J., Pen, U. 2002, *ApJ*, 567, L111
- Li-Xin, Li., 1998, *Gen. rel. Grav.*, 30, 497
- Longair, M.S., 2008, *Galaxy Formation.* (Springer Berlin, Heidelberg, New York)
- Navarro, J. F., Abadi, M. G., Steinmetz, M., 2004, *ApJ*, 613, L41
- Oepik, E. J., 1970, *Irish AJ*, 9, 211
- Okabe, T., Nishimichi, T., Oguri, M., Peirani, S., Kitayama, T., Sasaki, S., Suto, Y., 2018, *MNRAS*, 478, 1141
- Pajowska, P., Godłowski, W., Zhu Z. H., Popiela, J., Panko, E., Flin, P., 2019, *JPAC*, 02, 005,
- Panko, E., Flin, P., 2006, *J. of Astronomical Data*, 12, 1
- Paz, D. J., Staszyn, F., Padilla, N. D., 2008, *MNRAS*, 389, 1127
- Paz, D. J., Sgró, M. A., Merchan, M., Padill, N., 2011, *MNRAS*, 414, 2029
- Peebles, P.J.E., 1969, *ApJ*, 155, 393
- Peebles, P.J.E., Yu, J., T. 1970, *ApJ*, 162, 815
- Pereira, M. J., Bryan, G. L., Gill, S. P. D., 2008, *ApJ*, 672, 825
- Press, W. and Shechter, P. 1974, *ApJ*, 187, 425
- Romanowsky, A. J., Fall, S. M., 2012, *ApJS*, 203, 107
- Schäfer, B. M., 2009, *Int. J. Mod. Phys.*, 18, 173
- Schäfer, B. M., Merkel, P. M., 2012, *MNRAS*, 421, 2751
- Schmitz, D. M.; Hirata, C. M.; Blazek, J; Krause, E. 2018, *JCAP*, 07, 030
- Schneider, M.D., Bridle, S., 2010, *MNRAS*, 402, 2127
- Shandarin, S.F. 1974, *Sov. Astr.* 18, 392
- Shandarin, S. F., Zeldovich, Ya. B., 1989 *Rev. Mod. Phys.* 61, 185
- Shandarin, S.F., Habib, Sa., Heitmann, K., 2012, *Phys. Rev. D*, 85, 3005
- Silk, J. 1968, *ApJ*, 151, 459

- Shechter, P., 1976, ApJ, 203, 297
Springel, V., White, S. D. M., Tormen, G., Kauffmann, G., 2001, MNRAS, 328, 726-750
Springel, V. 2010, MNRAS, 401, 791
Stephanovich, V.A., Godłowski, W., 2015, ApJ, 810, 167
Stephanovich, V.A., Godłowski, W., 2017, Research Astron. Astrophys., 17, 119
Struble M., Rood H., 1999, AJSS, 125, 35
Sunyaev, A. R., Zeldovich, Ya. B., 1970, Astroph. Sp. Sci., 7, 3
Sunyaev, A. R., Zeldovich, Ya. B., 1972 A&A, 20, 189
Tovmassian, H. M., 2015, Astrophysics, 58, 471
Trujillo, I., Carretero C., Patri, G., 2006, ApJ, 640, L111
Varela, J., Betancort-Rijo, J., Trujillo, I., Ricciardelli, E., 2012, ApJ 744, 82
Vogelsberger, M., Genel, S., Sijacki, D., et al. 2013, MNRAS, 436, 3031
Wang, J., Tsang, W.W., Marsaglia, G. 2003, J. of Statistical Software, 8 (18), 1
Zhang, Y., Yang, X., Wang, H., Wang, L., Mo, H., van den Bosch, F., 2013, ApJ, 779, 160
Zeldovich, Ya. B., 1970, A&A, 5, 84
Zjupa, J., Springel, V., 2017, MNRAS, 466, 1625-1647

Uniwersytet Opolski, Institute of Physics, ul. Oleska 48, 45-052 Opole, Poland
(stef@uni.opole.pl).

Uniwersytet Opolski, Institute of Physics, ul. Oleska 48, 45-052 Opole, Poland (god-
lowski@uni.opole.pl).

Institute of Physics, Jan Kochanowski University, ul. Swietokrzyska 15, 25-406
Kielce, Poland.

Uniwersytet Opolski, Institute of Physics, ul. Oleska 48, 45-052 Opole, Poland.